Geophysical Surveys for Saltwater Intrusion Assessment Using Electrical Resistivity Tomography and Electromagnetic Induction Methods

Mansourian, D.[1] ✉ ⓘD | Hamidi, A.[2] ⓘD | Makarian, E.[3] ⓘD | Namazifard, P.[4] ⓘD | Mirhashemi, M.[5] ⓘD

1. **Corresponding Author**, Department of Geology and Environment, Faculty of Science, Ghent University, Ghent, Belgium. E-mail: dmansourian@yahoo.co.uk
2. Department of Geology, Faculty of Science, Ferdowsi University of Mashhad, Mashhad, Iran. E-mail: asiehhamidi@yahoo.com
3. Department of Petroleum Exploration, Faculty of Mining Engineering, Sahand University of Technology, Tabriz, Iran. E-mail: esmael.makarian@gmail.com
4. Department of Petroleum Exploration, Faculty of Mining Engineering, Sahand University of Technology, Tabriz, Iran. E-mail: pe_namazifard@sut.ac.ir
5. Department of Petroleum Exploration, Faculty of Mining Engineering, Sahand University of Technology, Tabriz, Iran. E-mail: mirhashemi.maryamm@yahoo.com

Abstract

Saltwater intrusion is as an environmental hazard in coastal lines if not appropriately managed. The over-exploitation, over-population and climate change have invited and pushed the saltwater landwards and polluted the freshwater aquifers. This research studies the results of the implemented project at the coast of Saint Andre' located in Koksijde, Belgium, to study this phenomenon through near-surface geophysics. Two geophysical methods, including Electrical Resistivity Tomography (ERT) and Electromagnetic Induction (EMI) were used to identify the saltwater intrusion. The present study aimed to investigate the possibility of saltwater intrusion, its extension and assess the government reclamation attempts to push back the saltwater. In the inversions, the Depth of Investigation Index (DOI) and the topography effect were evaluated. The subsurface conductivity of both methods was compared. The reliability of both methods to identify the saltwater intrusion has been established; however, the ERT survey provided a more comprehensive visualization than the EMI. The saltwater intrusion was found in the first 80 m of the coastal line with resistivity values of 2 to 5 Ohm.m; however, the infiltration of freshwater and the reclamation operation have stopped the further progress salinity into the dunes. Local possibilities of brackish water or clay lenses were identified with 7 to 25 Ohm.m resistivity values. The freshwater body was observed at distances between 120 and 220 m of the ERT line with values between 46 and 136 Ohm.m. The results were correlated with other studies, proving the reliability of the models.

Keywords: Electrical resistivity tomography, Electromagnetic induction, Reclamation, Depth of investigation index, Brackish water.

1. Introduction

In coastal unconfined aquifers, the freshwater discharges into the shallow seafloor. The saltwater in the sea and the fresh water in the aquifer collide with a sharp boundary developing due to the molecular diffusion and short-term tidal fluctuations. The fluctuations of the tides and freshwater head lead to the salt-fresh water interface shift towards or away from the sea, which forms saltwater intrusion in the case of the former (Fitts, 2002). The saltwater intrusion is recognized as an environmental hazard that threatens the quality of aquifers and water resources. The frequency of this phenomenon is severely more prominent in the coastal areas. The reason for this incident is the freshwater exploitation of the local industrial and urban lands close to the sea, which results in diminishing the water quality and unsustainable use of coastal resources such as land and stocks (Nowroozi et al., 1999). It is mostly due to the demand for freshwater resources that water extraction increases and saltwater intrusion occurs (Mtoni, 2013). The coastal areas are dynamic and interfaces between two different densities of saline water and freshwater. In saltwater intrusion, the interface between these two bodies of

water moves landwards, which results in the change of hydrological and environmental stability of the shore. The appropriate explanation for saltwater intrusion is found in the study of Allen & Matsuo (2002), in which they believe that the saltwater intrusion is the Dynamic equilibrium between the hydraulic gradient driving groundwater seaward and the hydraulic gradient emerging from the ocean in a landward direction. In summary, the excessive drainage of freshwater from the coastal aquifers, the increase of water demand and climate change are the significant factors that can easily lead to the intrusion of saltwater into the shore (Fennema & Newton, 1982; Werner et al., 2013; Barlow & Reichard, 2009). The rise of the sea level is another cause of the coastal saltwater intrusion, rapidly increasing due to the climate change. It could cause concern in certain geographical parts of the world, such as the North Sea and countries like the Netherlands, Belgium, and England (Essink, 2001; Nicholls, 2011). However, some studies suggest that the rise of seawater does not have a long-term effect on the saltwater intrusion of the coasts (Chang et al., 2011). The principle of Ghyben-Herzberg relation identifies this phenomenon and states that assuming no mixing between the saltwater and freshwater, for every foot above sea level, the freshwater head is stabilized and then extracted, the depth of sea water-freshwater interface will be 40 times larger. It indicates the 40-time stronger advancement of the saltwater into the shore for every unit volume of freshwater extraction. Since several studies attempt to address this issue (Kebede & Nicholls, 2010; Norconsult, 2007; Polemio et al., 2010; Mtoni et al., 2011; Papadopoulou et al., 2005), it is necessary to develop an objective approach to identify the extent of this problem in the coastal area. Saltwater intrusion can be studied using several methodologies, amongst which one can refer to: 1- Material analysis methods such as hydrological sampling and drilling; 2- Simulation technology based on runoff and historical data; and lastly 3-

Geoelectrical data acquisition (An et al., 2009; Nowroozi et al., 1999). Some studies, such as Mtoni (2013), state that a combination of hydrogeochemical and geophysical studies and modeling shall be considered a comprehensive methodology to address saltwater intrusion. Geophysics is widely used in hydrogeological studies to establish a link between the electrical properties of the formation and its fluid content (Zohdy et al., 1974). Due to the difference between freshwater and saltwater's electrical resistivity (ER), geophysical methods such as resistivity and electromagnetic have been often used for saltwater intrusion studies (Frohlich et al., 1994; Goodell, 1986; Flanzenbaum, 1986). Material resistivity depends on fluid salinity, fluid saturation, porosity and aquifer lithology (Lashkaripour et al., 2005). This parameter has been vastly implemented in the studies of many researchers to account for various problems (Walraevens et al., 1993; Obikoya & Bennell, 2012). The use of geophysical methods has always been a valuable approach in geological and engineering studies, gaining the attention and satisfaction of scientists. This is factual and remains so because geophysical methods investigate the earth in a short time and on large scales without physical disturbance. Thanks to the immense advance in science and technology, shallow geophysics surveys have been developed with 2D, 3D, and 4D spatial and temporal imaging abilities (Jongmans & Garambois., 2007). The mentioned methods have the advantages of being abrupt, deployable on slopes, and non-invasive; however, they might need certain calibration levels. Measuring the electrical conductivity can be a very good way of determining the quality of the groundwater. With any increase in the TDS values of the water, the salinity and electrical conductivity show fluctuations. Lebbe et al. (2011) formulated a categorization for the determination of groundwater salinity where he related the conductivity and TDS values of water to its salinity (Table 1).

Table 1. Salinity classification according to TDS and Conductivity values (Lebbe et al., 2011).

Salinity	TDS (mg/l)	Conductivity (mS/m)
Very Fresh	<200	<5
Fresh	200-400	5-10
Moderately Fresh	400-800	10-20
Low Fresh	800-1600	20-40
Moderately Brakish	1600-3200	40-80
Brakish	3200-6400	80-160
Very Brakish	6400-12800	160-320
Moderately Salie	12800-25600	320-640
Very Saline	>25600	>640

Similar to conductivity, its reverse parameter (resistivity) also plays a significant role in salinity classification. Identifying the electrical resistivity is a widely used geophysical method in shallow investigations (Telford et al., 1990), often used in saltwater investigations (Mtoni, 2013). The ER is a parameter that can identify different geological media and is effective for various surveys. In saltwater intrusion, the effect of salinity can be quite accurately determined using resistivity detection surveys such as electrical resistivity tomography (ERT). Walraevens et al. (1994) and De Moor & De Breuck (1969) stated that formation resistivities below 3.12 ohm.m are an indication of saltwater and below 12.5 ohms.m relate to brackish water (Table 2).

The ERT method, which seeks to depict the ER, is based on the differences in the amount of resistivity of the geological medium and carries certain robustness to electrical interfaces. It identifies both vertical and horizontal variations and, as a geo-electrical method, has a good capability to identify soil physical properties and can also be correlated with soil strength parameters and clay content (Jeřábek et al., 2017; Garcia-Tomillo et al., 2018; Maslakowski et al., 2014; Mansourian et al., 2020). It measures the potentials between one pair of electrodes while a direct current is transferred between another pair of electrodes. The depth of current influence is a factor of the electrode spacing and the configuration of the electrodes (Mtoni, 2013; Kirsch, 2009, George, 2006). Between several configurations that the ERT technique can have, the ideal array will be the one with a high resolution and high signal-to-noise ratio (Martorana et al., 2017).

Table 2. Relation of formation resistivity (ρ_t) and water resistivity (ρ_w) to groundwater quality and the groundwater classification of De Moor & De Breuck (1969) (Walraevens et al., 1994).

Schematic Subdivision		ρ_t (Ωm,11 ^{0}C)	ρ_w (Ωm,11 0C) ($\rho_w = \rho_t /4$)	Groundwater quality class
Fresh	Fresh	>200	>50	very fresh (VF)
		200-100	50-25	fresh (F)
		100-50	25-12.5	moderately fresh (MF)
		50-25	12.5-6.25	weakly fresh (WF)
	Brackish	25-12.5	6.2-3.13	moderately brackish (MB)
Salt		12.5-6.25	3.13-1.56	brackish (B)
	Salt	6.25-3.12	1.56-0.78	very brackish (VB)
		3.12-1.56	0.78-.0.39	moderately salt (MS)
		>1.56	>0.39	salt (S)

The gradient array, dipole-dipole, and the Schlumberger configurations are recommended by Dahlin & Zhou (2004). When looking at large anomalies, the difference between the configurations, as mentioned earlier, becomes insignificant. However, some configurations, such as dipole-dipole, can be more reliable when looking at small anomalies or thin interfaces (Mansourian et al., 2020; Salami, 2020). The use of the electromagnetic induction (EMI) approach is another additional method to investigate the subsurface. It can be used in several disciplines such as contamination studies, soil, agriculture, hydrology, etc. (Everett, 2012). It comprises a transmit coil that generates a primary electromagnetic field (by indirect alternating currents). The primary field causes eddy currents that manifest the secondary magnetic field identified with a receiver coil (Mansouian et al., 2020; George, 2006; Bell et al., 2001). For the particular EM34 device used in this study, two separated coils can be positioned vertically (Horizontal dipole) or horizontally (Vertical dipole). In the latter case, the depth of investigation will be extended. When the depth of the horizontal dipole is 15 m, the vertical dipole can investigate 30 m depth (McNeill, 1980).

Since the conductivity and resistivity are the reversed values of each other, they can easily be used in the same context, for example, soil water content, clay content, groundwater flow patterns and depth identification (Doolittle & Brevik, 2014). The sensitivity of the methods mentioned above (ERT and EMI) to water content and electrical conductivity has made them reliable methods for hydrological surveys (Romero-Ruiz et al., 2018). Still, there are several differences between the two discussed methods. EMI is a fast, non-invasive method and does not require ground contact, and depending on the case study, it does not necessarily require inversion for the results. On the other hand, the ERT is a multichannel contact approach that provides inverted profiles for the results. The inverted data provides better visualization of the results, leading to a more reliable subsurface interpretation (Mansourian et al., 2020). Since both methods evaluate the same parameter, an appropriate choice between the two can

partly depend on the user's preference. Toy (2015) clarified this and stated that both methods had equal reliability in qualitative data for studies related to water content, e.g. saltwater intrusion.

The problem of saltwater intrusion was investigated utilizing several geophysical methods. Since this problem can be resolved by several means, e.g. artificial recharge or change in water exploitation patterns (Abarca et al., 2006), it is helpful to temporally and spatially investigate it. Wiederhold et al. (2013) used ground-penetrating radar, seismic, ERT, and EMI to identify water lenses. However, in several studies, the ERT method, although having some depth limitations, has been proven as a very reliable approach for saltwater intrusion studies (Ronczka et al., 2015; Nguyen et al., 2009; Ogilvy et al., 2009; De Franco et al., 2009; Martinez et al., 2009; Zarroca et al., 2011). Geo-electrical methods are well suited for characterizing saltwater intrusion, which is because these methods are sensitive to ground conductivity and can depict the subsurface conductivity fluctuations that mostly occur due to a change in water content or salinity (Knight & Endres, 2005; Goldman & Kafri, 2006). Wiederhold et al. (2013) used surface and borehole ERT methods to investigate the saltwater intrusion, successfully imaged the salinity with an inversion model, and correlated the behavior with borehole and sampling data of fluid conductivity. De Franco et al. (2009) used the concept of ERT in a time-lapse fashion and analyzed the daily ERT tomograms of two different electrode spacings (2.5 and 5 m) close to a 12m thick phreatic aquifer. They depicted three consecutive aquifers down to 40 m depth. They managed to find the saltwater intrusion and a seasonal variation with a landward approach in winter and the opposite direction in summer. They related the summer drop of saltwater to the rainfall recharge of freshwater over the mainland. The latter scientist believes that saltwater has a dynamic behavior, and constant monitoring is vital in reclamation areas where recharge and discharge occur consecutively. This significance is also addressed in the study of Goebel et al. (2017). They carried out a comprehensive ERT survey on the coast of

California. They found significant saltwater intrusion and severe fluctuations that depended on several recharge zones or pumping wells. In this research, we carried out two geophysical surveys on a reclamation area on the coast of Belgium, using ERT and EMI techniques and attempted to depict the saltwater intrusion and visualize the spatial distribution of saltwater and freshwater in the region and compare the two methods in both accuracy and depth concerning their errors. The surveys were carried out, and the inversion detection methods were developed in a software. The saltwater intrusion was assessed qualitatively by visualization through ERT sections and quantitively by comparing with literature values. This project aimed to determine if the saltwater intrusion can be equally identified using both methods and comparing the two methodologies. The ERT technique and non-inverted EMI methods were compared to demonstrate the difference between the accuracy of the visualization. In addition, the success and failure of the reclamation project of the government were also assessed using both methodologies. The significance of this study lies within a comprehensive comparison between the two methods and the assessment of the depth of the investigation index (DOI), using the evaluation of the effect of topography in the ERT approach.

2. Study Area
2-1. Land use and General description
The project area is located on the coast of Belgium in Saint Andre's site in Koksijde and consists of two zones of extraction and infiltration. The extraction zone is where the fresh groundwater is pumped and extracted from the phreatic aquifer in the dunes. Since the dunes of the extraction site are in the vicinity of the Belgian coast, they are highly susceptible to saltwater intrusion originated from the North Sea and the Polder area. The pumping operations will therefore attract the saltwater towards the land, causing severe environmental problems. Due to the increase in the water demand and the rate of water extraction from the groundwater table in summer, a decline in the water level becomes evident, resulting in ecological problems emerging from the intrusion of saline water and drought. To achieve sustainable groundwater extraction for agricultural and urban use, the government constructed two infiltration lakes at Saint Andre's site to inject the treated (on-site) sewage water into the phreatic aquifer and keep the saltwater away from the dunes of the extraction site. The sewage water is picked over the surface water due to the negative impacts of the surface water infiltration on the environment and groundwater quality (Janssen, 1993).

Moreover, the closest surface water supply is located 6 km away from the project, which causes additional costs and jurisdictional problems that the sewage water treatment can easily be avoided. The lakes are 50 cm deep and 500 m long and are located between 40 and 100 m away from the extraction site (112 pumping wells). The land use is divided between the agricultural, recreational, natural reserve and residential areas with high water demand (Figure 1).
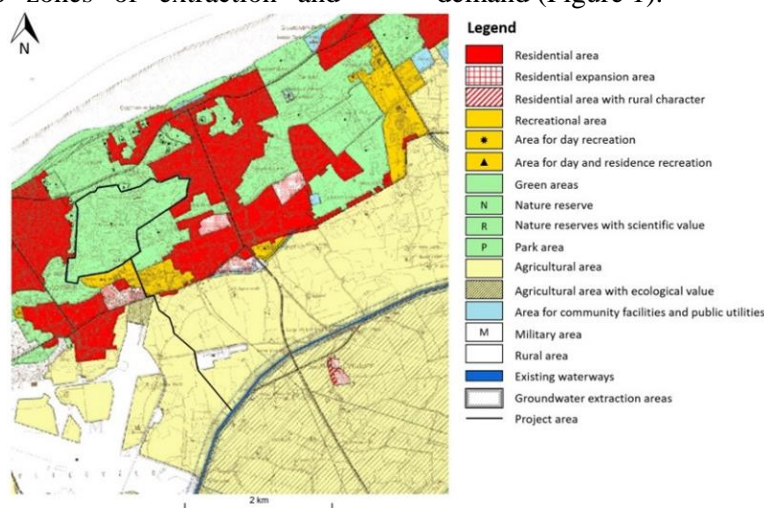

Figure 1. Regional land use plan.

Optimizing the infrastructure of water extractions: existing infrastructure for groundwater extraction (water-saving basins, pumping stations, etc.) must be optimized, considering the present nature- and landscape values, and agricultural potentials. For this reason, any underground survey that could inform the users of the subsurface conditions such as salinity and saltwater volume carries a significance that should not be overlooked.

2-2. Soil Properties

The soil type and relative soil properties are depicted in Figure 2. The soils are classified and characterized according to the Taxonomic Classification System from the DataBank Underground Vlaanderen (DOV) and WRB classification system. As demonstrated, the main soil fraction in the region is sand with 90% frequency content and increasing towards the sea. The soil has good permeability and not much fertility. The infiltration area is mainly on Arenosols with non-gravelly and moist sandy texture, with aeolian crossbedding and Calcaric properties and low nutrient evidence. The bulk density of the sandy soils is between 1.4 and 1.9 Mg/m^3 with 0.35 to 0.60 porosity, respectively, and the permeability of 1 m/day.

The entire area lies within two sections of the dunes and the polders with the infiltration and exploitation zones. The depth of the region varies between 6.58 m and 6.80 m TAW at the dunes and 7.5 m at the polders. Kortrijk is the primary form of dunes with 95 m thickness (Figure 3). It is a marine deposit formation made of clay with an approximate thickness of 100 m in the eastern Flanders. This formation is mainly impermeable and represents a well-defined threshold (Geets., 1988; Matthijs et al., 2013), considered the lower boundary of this study. This area comprises of one un-confined and one confined aquifer. The former is at the surface and 30 m thick, and the latter is deeper and 110- m wide.

2.3 Geophysical lines

The ERT and EMI lines were implemented perpendicular to the coastline after the infiltration and exploitation zones. Both lines covered the shore and the dunes with a comprehensive visualization of the aquifer (Figure 4).
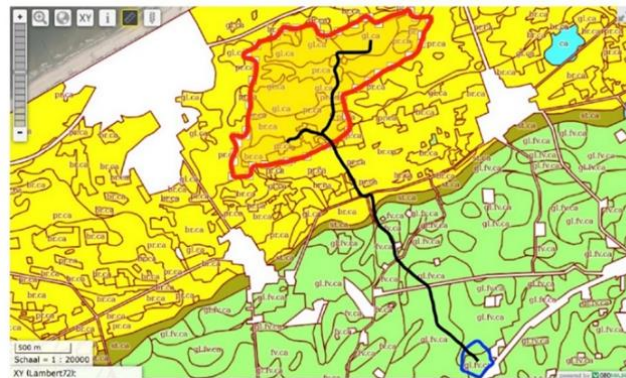

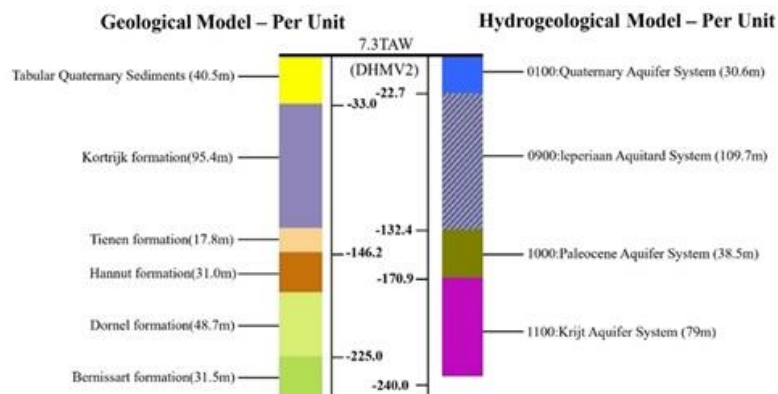**Figure 2.** The soil type of the project area (red zone indicates the infiltration zone).

Figure 3. The geological and hydrogeological models of the dunes.

(a)   (b)
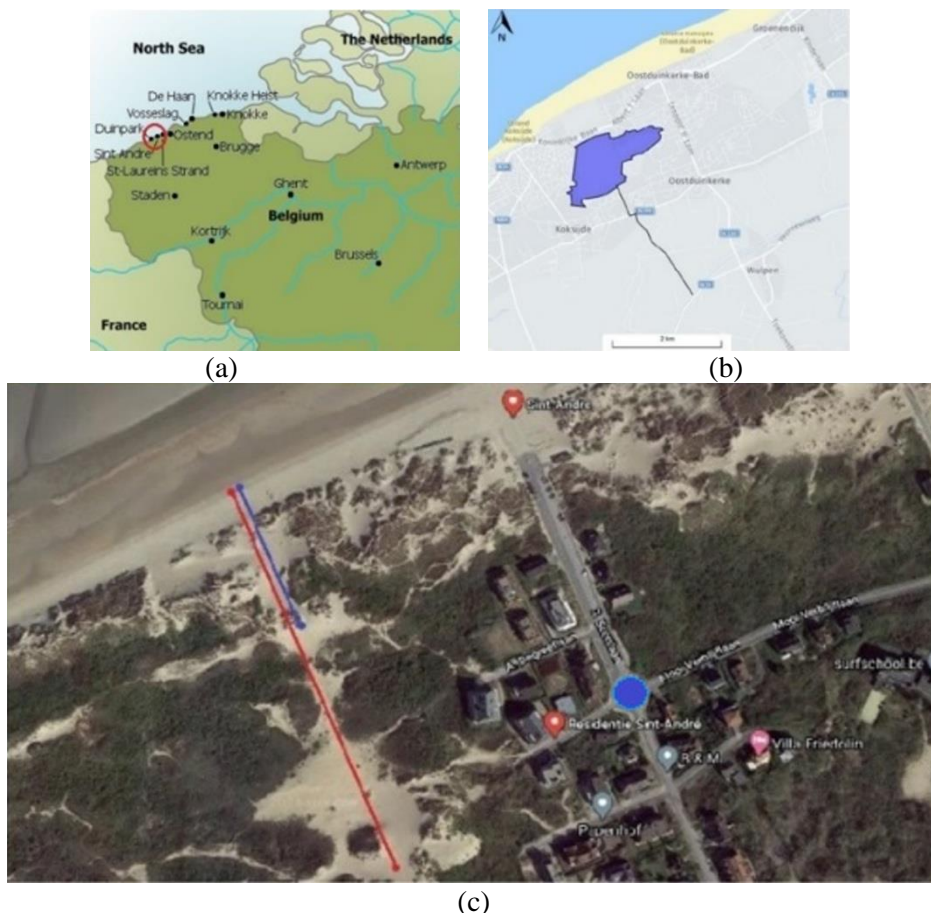

(c)

Figure 4. The study area in three different scales. a) represents the geographical location of the study area in Western Europe (Red Circle). b) represents the enlargement of the study area at the coast of Oostduinkerke with the infiltration zone located on top of the aquifer. The Geophysical lines (red line for ERT array and blue line for EMI) are depicted in (c). The Blue circle represents the location of the EM-39 study carried out by De Latte (2021).

3. Materials and Methods

The theoretical foundation of this study follows the equations of Archie's law, where he established a relationship between the bulk rock conductivity (σ_b) and water conductivity (σ_w) in porous media at variably saturated conditions.

$$\sigma_b = \frac{\Phi^m}{a} \sigma_w \times S^n \qquad (1)$$

where 'a' is the empirical constant =1, 'm' is the cementation exponent=1.2 to 4, which depends on the soil/rock type (Friedman, 2005), 'n' is the saturation exponent, which approximately equals 2, and "S" is the saturated fraction of the pore space (Φ).

To evaluate salinity in the region, assessing the electrical properties like conductivity was the most reliable method. Therefore, two geo-electrical surveys were implemented on the coast of Belgium to account for the saltwater intrusion. The measurements of the field were carried out, using a multielectrode system (Syscal Pro Switch from Iris instruments). The Syscal Pro is an all-in-one multinode resistivity and induced polarization imaging system for environmental geophysical studies. It includes a 10-channel receiver and a 250W, 2000Vpp internal transmitter that allows to perform up to 10 measurements at a time. The Syscal ERT system was powered by an external battery. The first survey was an ERT Schlumberger array with 10 m electrode spacing, from the shore to 320 m into the dunes and over the phreatic aquifer. The electrodes were inserted into the dry and loose sand and connected to the current wires (Figure 5). The EMI test was implemented using an EM34 device with 20 m inter coil spacing in horizontal dipole mode starting from the shore and continuing to 120 m on the dunes. The EM-34 device, with this

spacing of the coils in horizontal dipole mode, can reach 15 m of depth (Genotics limited Catalogue, 2017). While holding the dipoles, the applied induction steps of the EMI was 1 m. Considering that the phreatic aquifer is at a depth of 30 m, the implemented inter coil spacing and electrode spacing of the EMI and ERT methods made it possible to reach a suitable depth of investigation. The effect of the tide fluctuations was negligible in the results as both tests were approximately carried out simultaneously. The study area was cleared from any metallic objects that possess interference potential in the magnetic and electrical data acquisition. The ERT and EMI lines were situated away from fences and electrical towers to increase the data accuracy.

The RES2DINV software was used to analyze and model the ERT data as an inversion modeling approach to obtain a 2D inversion profile as a subsurface tomogram. RES2DINV is a computer program that automatically determines a two-dimensional (2-D) resistivity model for the subsurface for data obtained from 2-D electrical imaging surveys (Dahlin, 1996). The 2-D model used by the inversion program consists of many rectangular blocks that depend on the distribution of the data points in the pseudo section. The program uses a finite-difference or finite-element modeling procedure to calculate the apparent resistivity values. In addition, a non-linear smoothness constrained least-squares optimization technique is used to calculate the resistivity of the model blocks (De Groot-Hedlin & Constable, 1990). The interpretation of modeled apparent resistivity may be qualitative, which involves visual inspection of resistivity variation and anomalous occurrences (George, 2006). This image pictures the model of the difference between measured and calculated apparent resistivity (George, 2006; Loke & Barker, 1994). This software creates a 2D model, divides the subsurface into multiple rectangular blocks, and determines each block's resistivity. The program uses an inversion algorithm to adjust the resistivity of each block and minimize the difference between observed and calculated apparent resistivity. The initial model used in the software is usually a homogenous earth model. The program calculates the change in the model parameters that will reduce the difference between the calculated and measured apparent resistivity values. It adjusts the resistivity of the model blocks, subject to the smoothness constraints used. This difference is measured by the root-mean-squared (RMS) error. However, the model with the lowest possible RMS error sometimes shows large and unrealistic variations in the model resistivity values and might not always be the "best" model from a geological perspective. The best approach is to choose the model at the iteration, after which the RMS error does not change significantly. This usually occurs between the 3rd and 6th iterations (Geotomo Software, 2002). The depth of Investigation Index (DOI) and sensitivity were modeled along with topography.
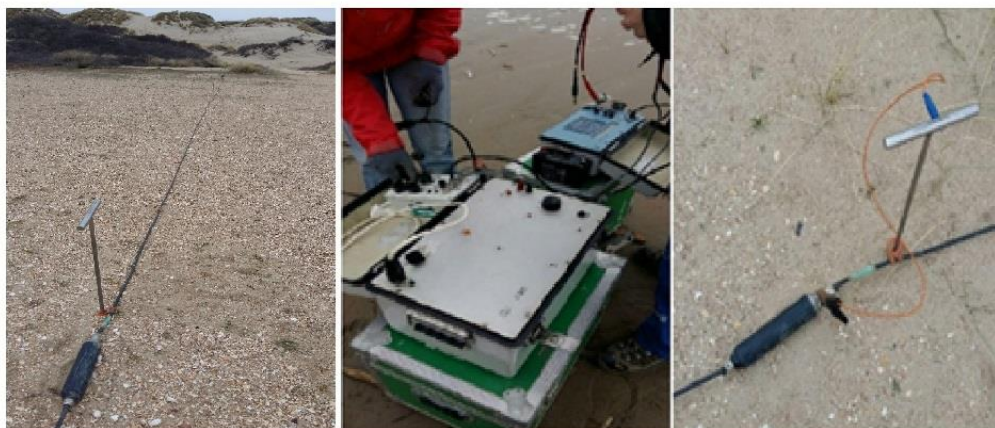

Figure 5. The ERT setup and electrode of the Schlumberger configuration.

In addition, the data was modeled for 10 m electrode spacing with the removal of bad data points to account for the variations of the error in the software. The apparent resistivity data was inverted, and the influence of topography, electrode spacing and DOI were evaluated in RES2DINV. The depth of the investigation refers to a threshold where the data is sensitive enough to interpret the inversion results. Below reliably, the information is not sensitive enough to pick the properties of the soil (Oldenburg & Li, 1999). Hence, the evaluation of this parameter is of paramount importance. Following Oldenburg & Li's (1999) method, the DOI was modeled and assessed in the software and compared with EMI results. Topographic data were measured on-site and entered into inversions for possible resistivity changes in the model due to the topographic effect. Besides, after removing the "bad data" points and obtaining a lower error rate, the RMS errors were plotted to account for the data accuracy and measurement quality. The profile models of the errors were also compared before and after the removal of the errors to assess the depth of the effect of the possible missing points in the inversions.

4. Results and Model Discussion
4-1. ERT Inversions (Resistivity)
4-1-1. Inversions without topography

Figure 6 represents the geophysical inversion of the Schlumberger configuration of the multichannel ERT survey with 10- m electrode spacing. The topographical data were not added to these profile sections to assume a smooth surface. The profiles embody the resistivity and sensitivity representations of the coast.

The figures demonstrate the resistivity variations of the coast and the dunes on the coast of Oostduinkerke in Belgium. The profile depicts the North Sea to the left of the top panel and signifies some small spatial distributions of low resistive zones across the line towards the dunes. The inversions cover more than 300 m in length, which are situated above the phreatic zone. The resistivity panel indicates that the saltwater has approached the coastal area to a certain extent. The shallow resistivity values (between 2 and 5 Ohm.m) have extended to approximately 100 m landwards. The profile indicates a trim level of saltwater intrusion in the region; however, this salinity has not been mixed with the aquifer and has not delivered a significant amount of low resistive saltwater into the dunes. These are the beneficial effects of the infiltration lakes injecting sewage water into the phreatic aquifer. The treated water has undoubtedly pushed the saltwater back towards the North Sea and reduced the level of saltwater intrusion.
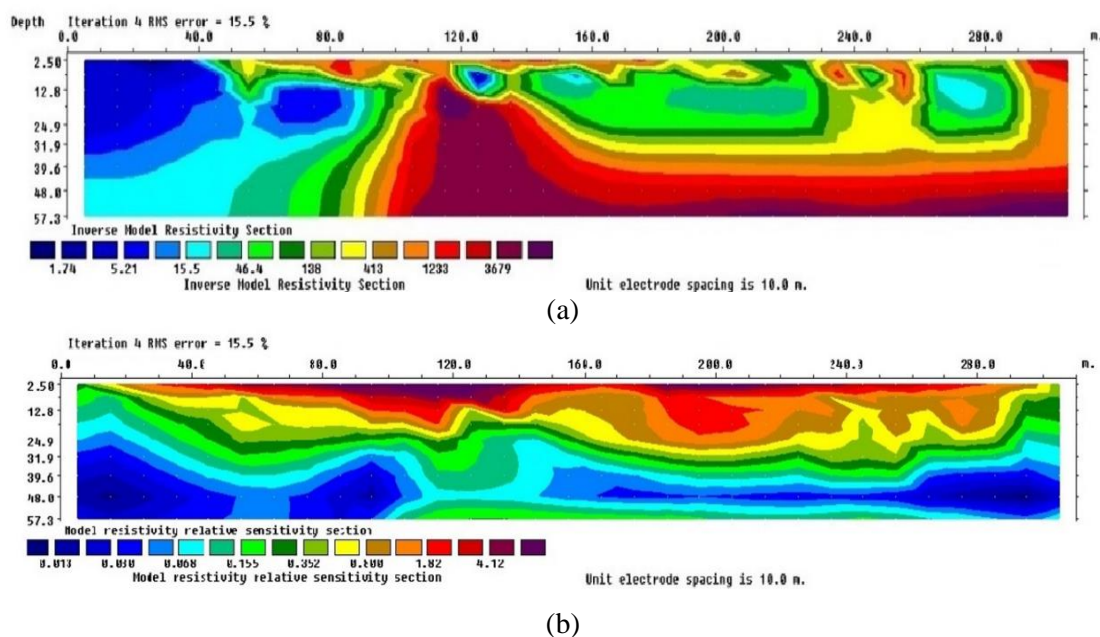

(a)

(b)

Figure 6. Inversions of the ERT method- Panel (a) shows the inverse resistivity and (b) represents the sensitivity section.

The local lenses of low resistivity can be evidence of remaining rain or brackish water or small clay lenses that will not cause concern. The values of resistivity observed in the inversion profile can also be a tool for identifying the saltwater and distinguishing between various bodies of water. According to Walraevens et al. (1994), the subsurface salinity can be determined by resistivity values below 12.5 ohms.m. It is also evident in the inversion profiles of the first 100 m of the survey line, where values start from app. 2 to 16 ohm.m. The transition between saltwater to freshwater passes through a phase of brackish water, which can be depicted by resistivity values between 6 and 25 ohms.m. This water phase can be found between 120 and 220 m of the survey line, manifested in small local water lenses. The possibility of small clay lenses is also considered as both bodies may appear with the same manifestation in the resistivity profiles. ER values above 50 ohms define the freshwater (green color), and their corresponding resistivities can be seen between 46 and 136 ohms.m under the dunes. The high resistivity values (above 3000 ohm.m) can be a representative of the Kortrijk formation. The quantity of current flowing into the subsurface quickly decreases with depth for a homogeneous ground. The sensitivity panel represents the spatially averaged quantity of currents and the near-surface resistivity distribution, which depends on the type of ERT configuration. The sensitivity function (S) defines the magnitude of the perturbation in the voltage. These plots give a good indication of the subsurface region to which a given measurement array is sensitive. This study shows that the profile is more sensitive, closer to the surface and the potential electrodes. It is true for Schlumberger configuration by the nature of the array (Everett, 2013). Note that the extent of the inversion profiles is already limited to the estimated depth of investigation being approximately 58 m (see DOI section).

4-1-2. Inversions with the topography

The topographical data was recorded at the site survey and added to the results. The height from the sea level maximizes at 10 m, with the highest points located at the dunes. Figure 7 represents the resistivity profile with topographical data. For these inversions, the field measurements of topography were added to the ERT data. The topographical variations were modeled in RES2DINV to account for the distortions of current flow lines due to the non-horizontal soil-air interface. The topography variations can impose a difference in the resistivity blocks, which is assessed in this section.
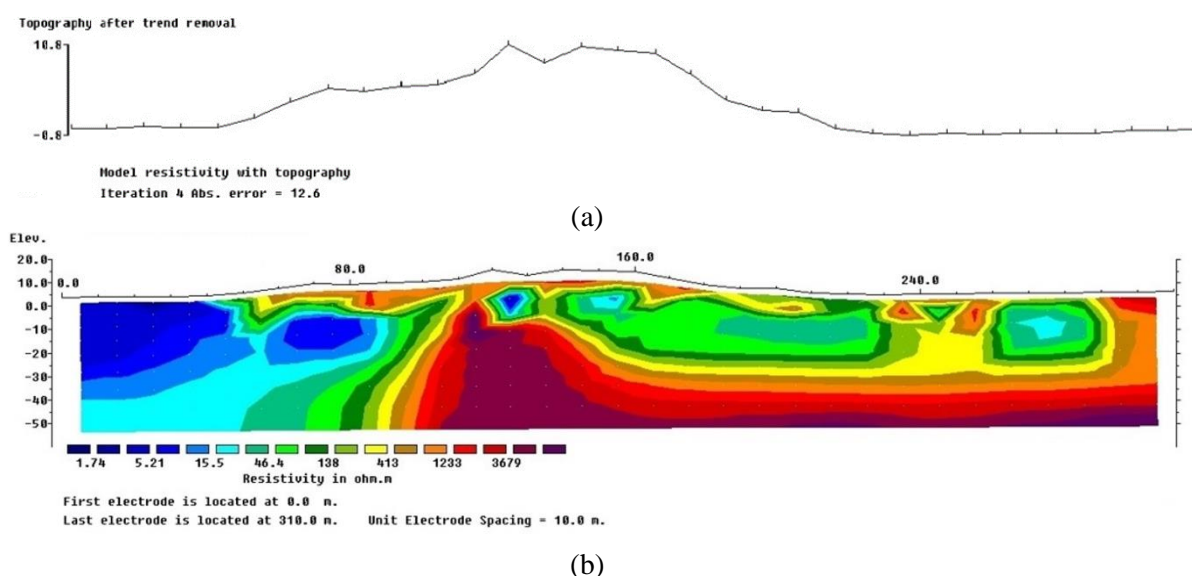

(a)

(b)

Figure 7. Topographical inversion of the study area: panel (a) trend of the topographical variations in the field; panel (b) the resistivity section with the effect of topography.

A comparison between Figures 7 and 6 shows that drastic changes cannot be seen when the topographical data is added to ERT results. However, small local variations can indeed be observed in some spots. The depth of the ERT survey is reduced by 7 m and reached 50 m. The extent of saltwater intrusion remain the same as in Figure 6. However, the absolute error (12.6%) indicates a 3% drop in the value. This means that adding the topographical data has indeed increased the accuracy of the model. A relatively high error in this area is due to the weak contact between the loose sand and the current electrodes inserted in the sand. Although the water was added to the location of the electrodes, the connection between the metallic pins and the sand prevented a great data acquisition. Any further attempts to manually reduce the absolute error would lead to a loss of important data and manipulate the model inversion. However, as indicated before, the lowest RMS error does not equal the best reliability (Geotomo Software, 2020). The objective was to achieve a minimum stable RMS error between iterations 3 to 6 without losing valuable data. This objective was successfully achieved, which confirms a reliable visualization of the models. The depth of the anomalies is approximately 2 m deeper without the effect of topography (Figure 6). The shape of some local anomalies over the dunes, this effect, however being insignificant, is still evident in specific locations, e.g. at 80-, 120- and 240-m length. At the highest elevation, approximately 10 m above the land surface, a relatively high resistive material can be seen with above 1000 ohm.m value related to the elevated dunes along the coast. Overall, a pronounced change in the inversion model is not observed due to the addition of topographical data yet the drop of error is visible.

4-1-3. Depth of Investigation Index (DOI)
After finalizing the inversions, the depth of investigation was modeled in RES2DINV following the Oldenburg and Li (1999) approach. They used two functions as data misfit and model misfit. The data misfit ensures that the final solution fits the observed data, and the model misfit describes the nature of the model and stabilizes the inversion to produce realistic results. They developed two inversions to find the DOI for different reference models. The processing of the calculation of the DOI index uses cells that extend to the ends of the survey line and a depth range of about three to five times the maximum median depth of investigation of the arrays in the data set. It ensures that data has minimal information about the resistivity of the cells near the bottom of the model, i.e. in theory, the bottom cells have DOI values of almost 1.0. However, if the model does not extend downwards sufficiently, the maximum DOI value might be much less than 1.0 (Geotomo Software, 2002). In this study, the approximation of the bottom DOI value (0.8) is acceptable. The reference model is usually a homogenous model with the average apparent resistivity value. In the DOI method, two inversions are carried out with different reference models, normally with 0.1 and 10 times the average apparent resistivity values. The DOI index will approach a value of 0.0 where the inversion produces the same cell resistivity values. However, regardless of the reference model resistivity, in areas well constrained by the data. It means more reliability for the data with smaller DOI index values (closer to 0.0). In areas with no information about the cell resistivity, this index will approach a value of 1.0 as the cell is similar to its reference resistivity. Thus, the model resistivity in areas where the DOI index has small values is considered reliable, while areas with high values are unreliable. Some model sections might have small local artifacts that might result in irregular DOI contours (Figure 8 middle panel). The 'Smoothed normalized DOI' display takes a weighted average of the DOI value for a particular model cell with the DOI values for the neighboring cells and attempts to remove and normalize the artifact (Geotomo Software, 2020). In this study, we followed this methodology, modeled the depth of investigation index and presented it in Figure 8.
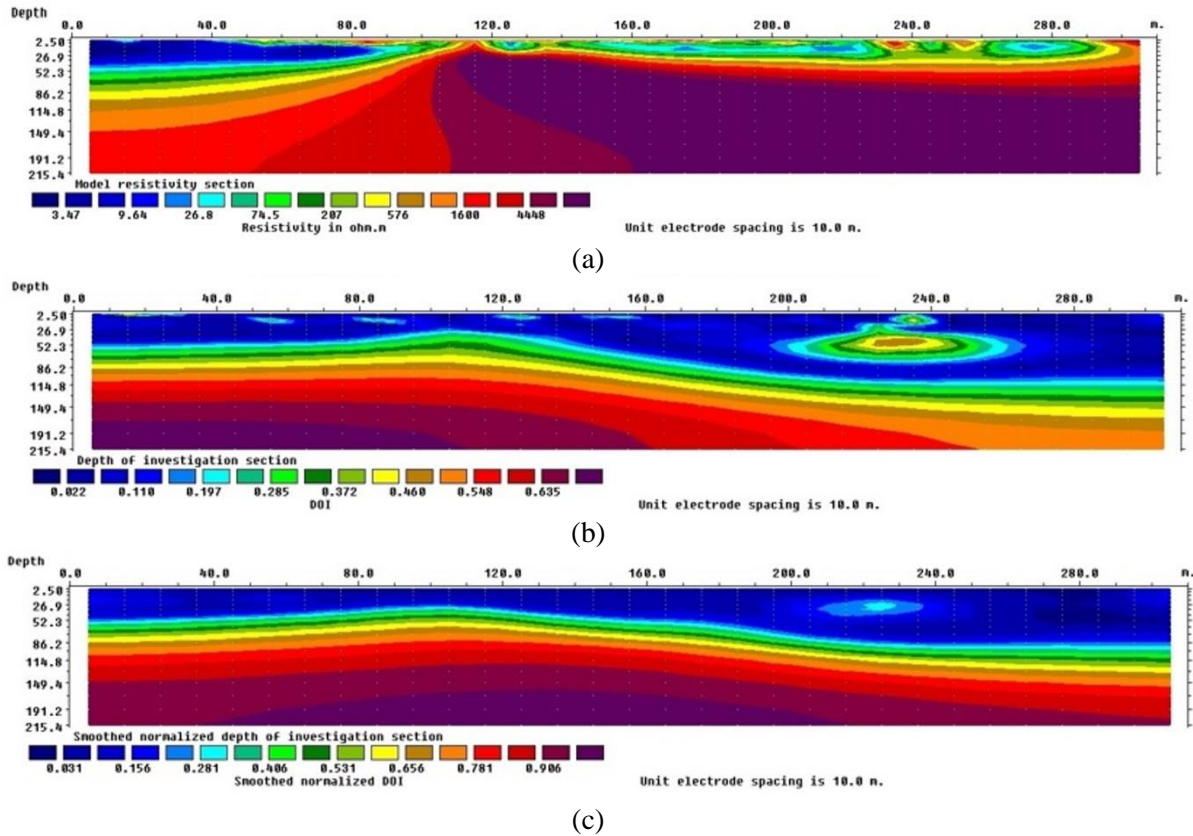
(a)

(b)

(c)

Figure 8. Depth of Investigation Index (DOI)- the panel (a) represents a larger scale of the resistivity section of the coast, with an extended depth of Figure 7. Panels (b) and (c) represent the DOI profile and variations.

The top section of Figure 8 shows the inverse resistivity model where the second reference model was used. As such, the inverse model values tend to be higher towards the bottom of the section as it trends to the reference resistivities used by the program. The middle section is the DOI section plot. If a DOI contour value of 0.4 is used as the cutoff point (the area which shows a rapid change of colors), the maximum depth of investigation in the middle of the survey line is about 60 m. The DOI panel of Figure 8 (middle panel) shows an abrupt increase in the DOI index, which occurs approximately at the vicinity of the green horizon (DOI ~ 0.4). Very thin layers can depict this abrupt increase. The homogenous dark blue horizon covering most surface layers is situated within the high sensitivity depth of investigation (DOI ~ 0.02). The multilayer nature of the bottom panel, below 60 m depth, indicates the lower accuracy of the survey at this depth. It is also inferred from the changing colors from dark and shallow blue (DOI ~ 0.02 to 0.26) to green and yellow (DOI ~ 0.03 to 0.6). This change in the color sequence is more abrupt compared

with the above 60 m. It means that the depth of investigation for this spacing and configuration is 60 m at the middle of the section, and below that, the results are not reliable. The reliability of the inversion remains only in the first 60-meter depth of the profile. This depth corresponds with the natural depth of the ERT survey that the software automatically picked to carry out the modeling (Figure 6). By calculating the smoothed normalized DOI, the problem of the artifact was solved, and it can be indicated that the DOI index values have not changed. It indicates that the artifact in the middle panel is an anomaly and must be disregarded. It is noteworthy that the evidence of the entire confined and unconfined aquifer under the dunes is observable in the top panel of Figure 8 (with purple and green colors) between 120- and 260-m lengths. The presumed aquifers are situated between 20- and 150-m depths, which correspond with the hydrological profile of the coast (Figure 3).

4-1-4. Inversion Errors
Starting from an initial model (usually a

homogenous earth model), we calculate the change in the model parameters using the program. That will reduce the difference between the calculated and measured apparent resistivity values. It adjusts the resistivity of the model blocks subject to the smoothness constraints used. A measure of this difference is given by the root-mean-squared (RMS) error. However, the model with the lowest possible RMS error can sometimes show large and unrealistic variations in the model resistivity values and might not always be the "best" model from a geological perspective. In general, the most prudent approach is to choose the model at the iteration, after which the RMS error does

not change significantly. This usually occurs between the 3rd and 6th iterations. Therefore, when the final models rests between iteration numbers 3 and 6, we can conclude that the model is reliable. Here, the data was displayed as a histogram and error plots (Figures 9a to 9d). The data points are grouped according to the difference between the measured and calculated apparent resistivity values. This option was utilized to remove the data points where a significant difference occurs. After removing the noisier data points, the inversions were carried out again with the trimmed data set to develop the prior presented models (Figures 6 to 8).
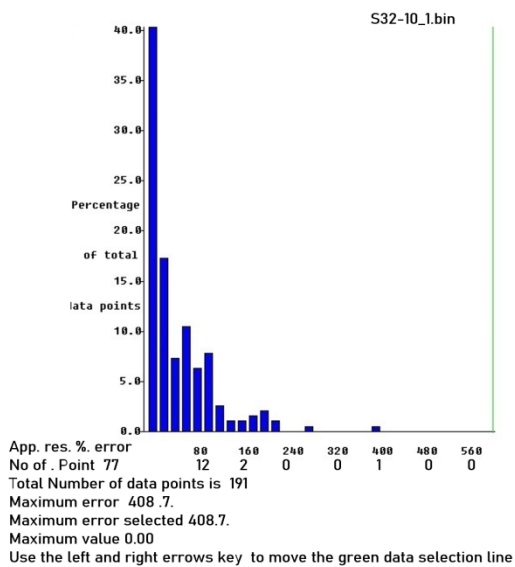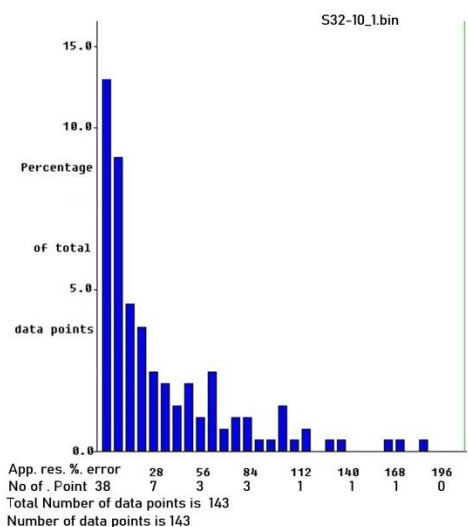

(a)
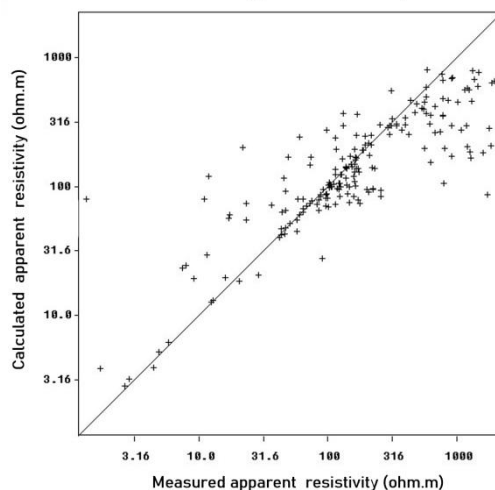
(b)

(c)
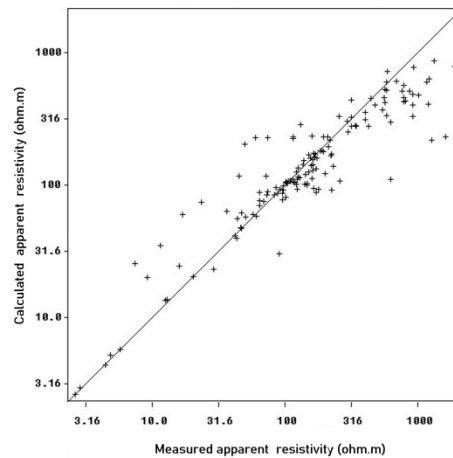
(d)

Figure 9. The histogram and RMS errors before and after the removal of bad data points: panels (a) and (b) show the status before removing the bad data points; and panels (c) and (d) demonstrate the status after the removal of bad data points.

In this study, due to the surface's texture and moisture content, which led to weak surface contact, the lowest possible error after the removal of bad data points, as demonstrated in the inversion profiles, was 12%. This weak contact resulted from the loose sandy material and the high saturation and precipitation of the coastal material at the time of the survey. It is noteworthy that in the next section, the EMI results can confirm the reliability of the ERT results.

4-2. Conductivity
4-2-1. EM-34 results
The electromagnetic induction methods was

carried out to assist and validate the ERT result's interpretation. Figure 10 represents the conductivity values measured by the EM34 device. Due to the shorter survey line of the EMI compared with the ERT, the plausible comparison of the data relies on the first 110 m of both surveys. For a more accurate comparison with the ERT, the conductivity values of the ERT survey line were extracted in the first 120 m of the survey line. The values of three depths of 12, 15, and 20 m were averaged and compared with the EMI device's conductivity values, which related to the depth of approximately 15 m.
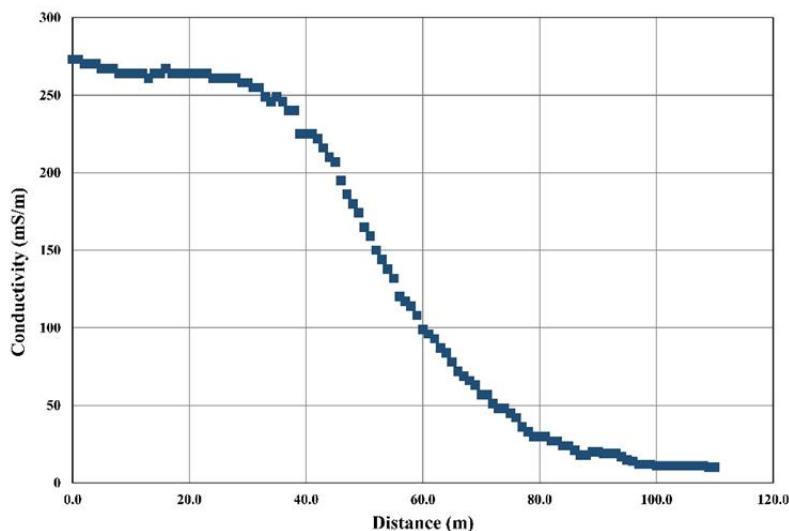

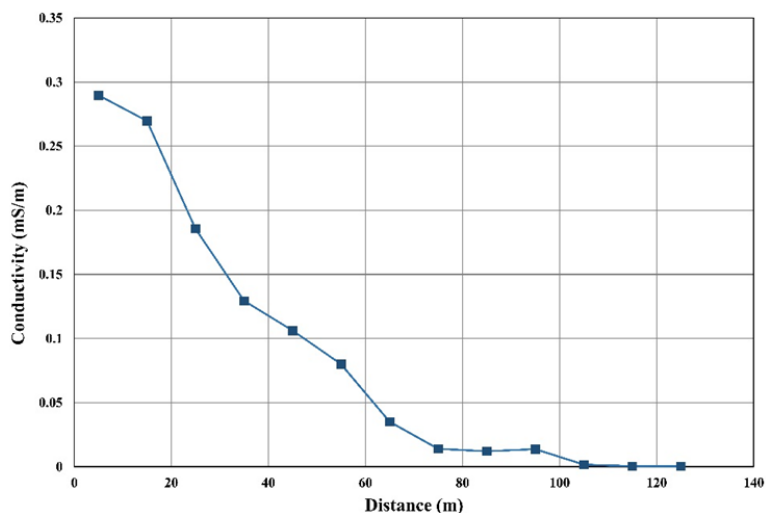**Figure 10.** Conductivity values of the coast measured by EM34 device.

Figure 11. Average Conductivity values extracted from ERT survey (N=3).

4-2-2. EM-39 results

In order to further validate the results of the ERT tests the results of both EM-34 and ERT surveys were correlated with the studies of De Latte (2021) when he carried out a study using the EM-39 device inside the boreholes in the dunes of the study area. The presented conductivity profiles (Figure 12) correspond to 100 to 120 m distance of the ERT arrays of this study (Figure 4). Based on Figure 12, the entire interval is occupied with semi-fresh water; however, the measurements are disturbed by the unsaturated sediments at the top layer (De Latte, 2021).

The result of the EMI validated the result obtained from the ERT. A very high conductive material related to saltwater was found at the beginning of the induction measurement. Comparing Figure 10 and Figure 6 informs us that both methods have successfully identified the saltwater body at the root of their survey lines. The general descending trend of the EMI values shows that the saltwater intrusion does not advance the first 60 m of the coast. Such a fact is also evident in the ERT inversion. However, due to the better visualization of the ERT and more data density of this method, the accuracy of the results is much more reliable than the EM34. Figure 11 shows that the average conductivity values extracted from the ERT data follow a similar trend to the EMI device. Both lines of Figures 11 and 10 have a descending pattern yet with different quantities. It is due to the averaged nature of the ERT extracted data (Figure 11) and that the EMI results are not inverted. In addition, the study of De Latte (2021) demonstrates similar values to the EM34 at approximately 100 m distance from the starting line, as both studies show a variation of approximately 20 mS/m. Both EMI surveys depict a transition of borderline saline water, at the coast, to fresh water (Table 1) at the dunes, with a drop of conductivity from 300 mS/m to 20 mS/m. These results can also be correlated with Table 2 and Resistivity data, where the values of resistivity increase from 2 ohm.m at the coast and elevate to 400 ohm.m after the dunes. Therefore it can be concluded that all the three surveys are reliable and their provided results are acceptable.

4-3. Resistivity and Sensitivity of Blocks

The resistivity and sensitivity data of the resistivity blocks were extracted from the field data (of the ERT measurements) and plotted in graphs to compare with the visual results of the ERT. Figure 13 represents the variations of the parameters as mentioned above with depth.
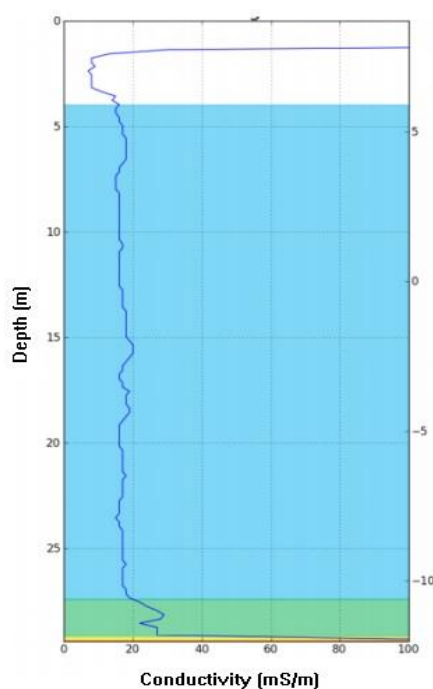

Figure 12. Borehole EM-39 Results (De Latte, 2021)- representing a borehole in the zone of saline water and freshwater interface.
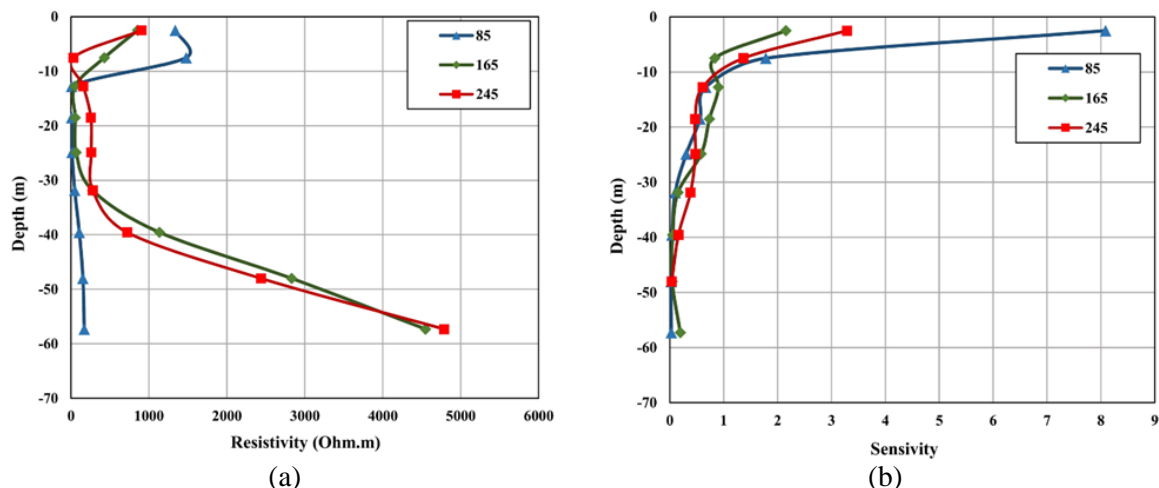
Figure 13. (a) Resistivity and (b) Sensitivity variations versus depth in three particular locations of the survey line.

Figure 13-a, shows the variations of resistivity in response to depth in three locations of the ERT line. They include 85, 165 and 245 m, corresponding to the left, top, and right dunes. Besides, the graph indicates a significant amount of drop-in resistivity after -10m. The resistivity value under 85 m point indicates that this location is situated over the saltwater. However, at 165 and 245 m, the values of resistivity increase successively and show a sudden increase deeper than -30 m. It shows a shallower yet less conductive anomaly in this region. These two points correspond to the freshwater aquifer of the area and possible clay lenses in the dunes. Also, Figure 13-b presents the sensitivity values of the same three points as the left image. It shows that the sensitivity drops below -10 m and continues until the depth of investigation (57 m) and proves that the sensitivity decreases with depth.

5. Conclusions

After the detailed analysis of the ERT and EMI data, the saltwater intrusion was detected on the coast of Oostduinkerke in Belgium. The increase in water demand and excess water extraction is the saltwater's cause of approaching the phreatic aquifer. This phenomenon is visible in the first 60 to 80 m of the coast with ERT and EMI measurements. The ERT method found the saltwater with resistivity below 7 ohms.m. The same location was identified as saltwater with non-inverted EMI results to conductivity above 250 mS/m. However, because of Flemish's government efforts, the advancement of the salinity and its progress

to becoming an environmental hazard were prevented. The infiltration lakes constructed in the vicinity of the project area have pushed the saltwater back and stabilized its status. Evidence of brackish water and possible clay lenses have been observed in the area. Besides, the freshwater was identified between 120 and 220 m of the survey line with resistivity values between 46 and 136 ohms.m. The topographical data of the ERT did not have a significant influence on the inversion results. The depth of investigation in which the data can be perfectly trusted is approximately 57 m in this project. Both ERT and EMI devices successfully identified the saltwater. Although averaged between three depths, the conductivity values extracted from the ERT still demonstrated a similar pattern to the EMI graph. It proves that both methods depict identical variations in the subsurface conductivities of the study area. However, due to the nature of the ERT and the non-inverted results, it is evident that the ERT results are more accurate and provide a more reliable visualization. The RES2DINV software successfully carried out the inversion. The error of the models could not be lower due to the bad ground contact between the soil particles and the electrodes and remained at the lowest possible value of 12.6%.

in the field work of this scientific paper.

References

Abarca, E., Vázquez-Suñé, E., Carrera, J., Capino, B., Gámez, D., & Batlle, F. (2006). Optimal design of measures to correct seawater intrusion. *Water Resour. Res.*, 42, http://dx.doi.org/10.1029/2005WR004524

Allen, D.M., & Matsuo, G.P. (2002). *Results on the Groundwater Geochemistry Study on Hornby Island*, British Columbia. Burnaby, B.C., Simon Fraser University. p. 9-12.

An, Q., Wu, Y., Taylor, S., & Zhao, B. (2009). Influence of the Three Gorges Project on saltwater intrusion in the Yangtze River Estuary. *Environmental Geology*, 56(8), 1679-1686.

Barlow, P.M., & Reichard, E.G. (2009). Saltwater intrusion in coastal regions of North America. *Hydrogeol. J.*, 18, 247–260., http://dx.doi.org/10.1007/s10040-0090514-3.

Bell, T.H., Barrow, B.J., & Miller, J.T. (2001). Subsurface discrimination using electromagnetic induction sensors. *IEEE transactions on geoscience and remote sensing*, 39(6), 1286-1293.

Chang, S.W., Clement, T.P., Simpson, M.J., & Lee, K.K. (2011). Does sea-level rise have an impact on saltwater intrusion?. *Advances in water resources*, 34(10), 1283-1291.

Dahlin, T., & Zhou, B. (2004). A numerical comparison of 2D resistivity imaging with ten electrode arrays. Geophysics. Prospect. 52(5), 379–398, http://dx.doi.org/10.1111/j.1365-2478.2004.00423.x.

Dahlin, T. (1996). 2D resistivity surveying for environmental and engineering applications. *First Break*, 14. 275-284.

De Franco, R., Biella, G., Tosi, L., Teatini, P., Lozej, A., Chiozzotto, B., Giada, M., Rizzetto, F., Claude, C., Mayer, A., Bassan, V., & Gasparetto-Stori, G. (2009). Monitoring the saltwater intrusion by time-lapse electrical resistivity tomography: The Chioggia test site (Venice Lagoon, Italy). *Journal of Applied Geophysics*, 69(3-4), 117-130.

DeGroot-Hedlin, C., & Constable, S. (1990). Occam's inversion to generate smooth, two-dimensional models form magneto telluric data. *Geophysics*, 55, 1613-1624.

De Latte., S. (2021). Characterisation of the saltwater/freshwater interface between Koksijde and Oostduinkerke using electrical resistivity tomography. Master's thesis. University of Ghent.

De Moor, G., & De Breuck, W. (1969). De freatische waters in het Oostelijk Kustgebied en in de Vlaamse vallei. *Natuurwet. Tijdschr.*, 51(1-2), 3-68, + 8 annexes.

Doolittle, J.A., & Brevik, E.C. (2014). The use of electromagnetic induction techniques in soils studies. *Geoderma*, 223, 33-45.

Essink, G.H.O. (2001). Saltwater intrusion in a three-dimensional groundwater system in the Netherlands: a numerical study. *Transport in porous media*, 43(1), 137-158.

Everett, M.E. (2013). Near-surface applied geophysics. Cambridge University Press.

Everett, M.E. (2012). Theoretical developments in electromagnetic induction geophysics with selected applications in the near-surface. *Surveys in geophysics*, 33(1), 29-63.

Fennema, R.J., & Newton, V.P. (1982). Ground Water Resources of the Eastern Shore of Virginia. Commonwealth of Virginia, State Water Control Board, Richmond, VA, Planning Bulletin, 332, 74 pp.

Fitts, C.R. (2002). *Groundwater science*. Elsevier.

Flanzenbaum, J. (1986). *Evaluation of saltwater intrusion into the Coastal Aquifer of Southern Virginia*. M.Sc. Thesis, University of Virginia, 141 p.

Friedman, S.P. (2005). Soil properties influencing apparent electrical conductivity: a review. *Computers and Electronics in Agriculture*, 46(1-3), 45-70.

Frohlich, R.K., Urish, D.W., Fuller, J., & Reilly, M.O. (1994). Use of geoelectrical method in groundwater pollution surveys in a coastal environment. *Journal of Applied Geophysics*, 32, 139–154.

García-Tomillo, A., de Figueiredo, T., Dafonte, J.D., Almeida, A., & Paz-González, A. (2018). Effects of machinery trafficking in an agricultural soil assessed by Electrical Resistivity

Tomography (ERT). *Open Agriculture*, 3(1), 378-385.

Geets, S. (1988). Ieper Groep. In: Mar_echal, R. & Laga, P., Voorstel Lithostratigra_sche Indeling van het Paleogeen. Nationale Commissies voor Stratigra_e, pp. 81-115.

Genotics limited catalogue (2017). Geophysical Instrumentation for Exploration & the Environment.

George, A. (2006). Development of geoelectrical techniques for investigation and monitoring of landfills. Cardiff University (United Kingdom).

Geotomo Software (2002), Rapid two-dimensional resistivity and induced polarization inversion using the least-squares method. RES2DINV manual.

Geotomo Software (2020), Rapid two-dimensional resistivity and induced polarization inversion using the least-squares method. RES2DINV manual.

Goebel, M., Pidlisecky, A., & Knight, R. (2017). Resistivity imaging reveals a complex pattern of saltwater intrusion along the Monterey coast. *Journal of Hydrology*, 551, 746-755.

Goldman, M., & Kafri, U. (2006). Hydrogeophysical applications in coastal aquifers. *In: Appl. Hydrogeophys. Springer*, Netherlands, pp. 233–254.

Goodell, H.G. (1986). A study of saltwater intrusion into the surface aquifer and the underlying of Yorktown Aquifer of Coastal Virginia. *Final Report to Virginia Environmental Endowment Richmond*, VA, 14 pp.

Janssen, M.P.J.M. (1993). Duinen voor de wind: Past (diep) in_ltratie in het streefbeeld van natuurontwikkeling?. *H2O*, (26), 388-393.

Jeřábek, J., Zumr, D., & Dostál, T. (2017). Identifying the plow pan position on cultivated soils by measurements of electrical resistivity and penetration resistance. *Soil and Tillage Research*, 174, 231-240.

Jongmans, D., & Garambois, S. (2007). Geophysical investigation of landslides: a review. *Bulletin de la Société géologique de France*, 178(2), 101-112.

Kebede, S.A., & Nicholls, J.R. (2010). *Population and assets exposed to coastal flooding in Dar es Salaam (Tanzania): vulnerability to climate extremes*. University of Southampton, United Kingdom. http://www.tzdpg.or.tz/uploads/media/Dar es Salaam_City-Analysis_Final-Report_1_.pdf

Kirsch, R. (2009). Petrophysical Properties ofPermeable and Low Permeable Rocks. In: *Groundwater Geophysics*: Tool for Hydrogeology, Kirsch, R. (Ed.). 2nd Edn., Springer, Berlin, Heidelberg.

Kight, R., & Endres, A.L. (2005). An introduction to rock physics principles for near-surface geophysics. In: *Near-Surface Geophysics*. Society of Exploration Geophysics, Tulsa, pp. 31–70.

Lashkaripour, Ghafoori, M., & Dehghani, A. (2005). Electrical resistivity survey for predicting Samsor aquifer properties, southeast Iran. *Geophysical Research Abstracts* (7) (Europian Geosciences Union).

Lebbe, L., Vandenbohede, A., & Courtens, C. (2011). Grondwaterstudie in kader van uitbreiding van het Zwin.

Loke, M.H., & Barker, R.D. (1994). Rapid least-squares inversion of apparent resistivity pseudo sections. In 56th EAEG Meeting (pp. cp-47). European Association of Geoscientists and Engineers.

Mansourian, D., Cornelis, W., & Hermans, T. (2020). Exploring geophysical methods for mapping soil strength in relation to soil compaction. Master's thesis. Ghent University.

Martínez, J., Benavente, J., García-Aróstegui, J.L., Hidalgo, M.C., & Rey, J. (2009). Contribution of electrical resistivity tomography to the study of detrital aquifers affected by seawater intrusion–extrusion effects: The river Vélez delta (Vélez-Málaga, southern Spain). *Eng. Geol.*, 108, 161–168, http://dx.doi.org/10.1016/j.enggeo.2009.07.004.

Martorana, R., Capizzi, P., D'Alessandro, A., & Luzio, D. (2017). Comparison of different sets of array configurations for multichannel 2D ERT acquisition. *Journal of Applied Geophysics*, 137, 34-48.

McNeill, J.D. (1980). Electrical conductivity

of soils and rock. Technical Note TN-5. Geonic Limited, Mississauga, Ontario, Canada.

Maślakowski, M., Kowalczyk, S., Mieszkowski, R., & Józefiak, K. (2014). Using Electrical Resistivity Tomography (ERT) as a tool in geotechnical investigation of the substrate of a highway. *Studia Quaternaria*, 31(2), 83-89.

Matthijs, J., Lanckacker, T., De Koninck, R., Deckers, J., Lagrou, D., & Broothaers, M. (2013). Geologisch 3D lagenmodel van Vlaanderen en het Brussels Hoofdstedelijk Gewest { versie 2, G3Dv2 [online]. Studie uitgevoerd door VITO in opdracht van de Vlaamse overheid, Departement Leefmilieu, Natuur en Energie, Afdeling Land en Bodembescherming, Ondergrond, Natuurlijke Rijkdommen, 21p., VITO-rapport 2013/R/ETE/43. [Accessed November 5th, 2019]. Available at: https://www.dov.vlaanderen.be (in Dutch).

Mtoni, Y., Mjemah, I.C., Van Camp, M., & Walraevens, K. (2011). Enhancing Protection of Dar es Salaam Quaternary Aquifer: Groundwater Recharge Assessment. Springer, Environmental Earth Sciences, *Advances in Research of Aquatic Environment*, (1), 299-306 (DOI 10.1007/978-3-642-19902-8).

Mtoni, Y.E. (2013). Saltwater intrusion in the coastal strip of Dar es Salaam Quaternary aquifer, Tanzania (Doctoral dissertation, Ghent University).

Nguyen, F., Kemna, A., Antonsson, A., Engesgaard, P., Kuras, O., Ogilvy, R., Gisbert, J., Jorreto, S., & Pulido-Bosch, A. (2009). Characterization of seawater intrusion using 2D electrical imaging. *Near Surf. Geophys.*, 7, 377–390.

Nicholls, R.J. (2011). Planning for the impacts of sea-level rise. *Oceanography*, 24(2), 144-157.

Norconsult (2007). Development of a Future Water Source for Dar es Salaam, Tanzania. Pre-design and Environmental report, Phase 2. Part 2: Review of Social and Environmental Factors.

Nowroozi, A.A., Horrocks, S.B., & Henderson, P. (1999). Saltwater intrusion into the freshwater aquifer in the eastern shore of Virginia: a reconnaissance electrical resistivity survey. *Journal of Applied Geophysics*, 42(1), 1-22.

Obikoya, I.B., & Bennell, J.M. (2012). Geophysical investigation of fresh-saline water interface in the coastal area of Abergwyngregyn. *Journal of Environmental protection*, 3, 1039-1046.

Ogilvy, R.D., Meldrum, P.I., Kuras, O., Wilkinson, P.B., Chambers, J.E., Sen, M., Pulido-Bosch, A., Gisbert, J., Jarrett, S., Frances, I., & Tsourlos, P. (2009). Automated monitoring of coastal aquifers with electrical resistivity tomography. *Near Surf. Geophys.*, 7, 367–375.

Oldenburg, D.W., & Li, Y. (1999). Estimating depth of investigation in dc resistivity and IP surveys. *Geophysics*, 64(2), 403-416.

Papadopoulou, M.P., Karatzas, G.P., Koukadaki, M.A., & Trichakis, Y. (2005). Modeling the saltwater intrusion phenomenon in coastal aquifers – a case study in the industrial zone of Herakleto in Crete. *Global NEST Journal.* 7(2), 197-203.

Polemio, M., Casarano, D., & Limoni, P.P. (2010). Apulian coastal aquifers and management criteria In: *SWIM 21 - 21st Salt Water Intrusion Meeting*. Edited by: MT Condesso de Melo, L Lebbe, JV Cruz, R Coutinho, C Langevin, A Buxo, 203-206.

Romero-Ruiz, A., Linde, N., Keller, T., & Or, D. (2018). A review of geophysical methods for soil structure characterization. *Reviews of Geophysics*, 56(4), 672-697.

Ronczka, M., Voß, T., & Günther, T. (2015). Cost-efficient imaging and monitoring of saltwater in a shallow aquifer by using long electrode ERT. *Journal of Applied Geophysics*, 122, 202-209.

Salami, O. (2020) *Evaluation of soil compaction of an agricultural field using 2D electrical resistivity tomography (ERT)*. Master's thesis. University of Gent.

Telford, W.M., Geldart, L.P., Sherif, R.E., & Keys, D.A. (1990). Applied geophysics. Cambridge Univ. Press, Cambridge, 770p.

Toy, C. (2015). *Monitoring Shallow Vadose Zone Moisture Dynamics using Electrical Resistivity Tomography and*

Electromagnetic Induction (M.Sc. thesis, University of Waterloo).

Werner, A.D., Bakker, M., Post, V.E.A., Vandenbohede, A., Lu, C., Ataie-Ashtiani, B., Simmons, C.T., & Barry, D.A. (2013). Seawater intrusion processes, investigation, and management: recent advances and future challenges. *Adv. Water Resour.*, 51, 3–26.

Walraevens, K., Lebbe, L., Van Camp, M., Angius,, Serra, M.A., Vacca,, A., Massidda, R., & De Breuck, W. (1993). Salt/freshwater flow and distribution in a cross-section at Oostduinkerke (western coastal plain of Belgium). *Study and modeling of Saltwater Intrusion into Aquifers.* Proceedings of 12th Saltwater Intrusion.

Walraevens, K., Martens, K., & De Breuck, W. (1994). Salt/freshwater distribution in the polder area near Axel (Zealand-Flanders). *Proceedings of the 13th Salt-Water Intrusion Meeting*, *Cagliari (1994),* 321-334.

Wiederhold, H., Sulzbacher, H., Grinat, M., Günther, T., Igel, J., Burschil, T., & Siemon, B. (2013). Hydrogeophysical characterization of fresh-water/saltwater systems — case study: Borkum Island, Germany. *First Break*, 31, 109–117.

Zarroca, M., Bach, J., Linares, R., & Pellicer, X.M. (2011). Electrical methods (VES and ERT) for identifying, mapping, and monitoring different saline domains in a coastal plain region (Alt Empordà, Northern Spain). *J. Hydrol.*, 409, 407–422, http://dx.doi.org/10.1016/j.jhydrol.2011.08.052.

Zohdy, A.A.R., Eaton, G.P., & Mabey, D.R. (1974). Application of surface geophysics to groundwater investigation, U.S.G.S. Techniques of Water-Resource Investigation, Book 2.